Structure–activity relationships of synthetic cannabinoid designer drug RCS-4 and its regioisomers and C4 homologues

Samuel D. Banister, Jordyn Stuart, Trent Conroy, Mitchell Longworth, Madhura Manohar, Corinne Beinat, Shane M. Wilkinson, Richard C. Kevin, David E. Hibbs, Michelle Glass, Mark Connor, Iain S. McGregor, Michael Kassiou

Published: 31 May 2015

by Springer

in Forensic Toxicology

Forensic Toxicology, Volume 33, pp 355-366; doi:10.1007/s11419-015-0282-9

Structure-activity relationships of synthetic cannabinoid designer drug RCS-4 and its regioisomers and C4-homologues

Samuel D. Banister[1,2] · Jordyn Stuart[3] · Trent Conroy[2,4,5] · Mitchell Longworth[2] · Madhura Manohar[2] · Corinne Beinat[1,2] · Shane M. Wilkinson[2] · Richard C. Kevin[6] · David E. Hibbs[7] · Michelle Glass[8] · Mark Connor[3] · Iain S. McGregor[6] · Michael Kassiou[2,9]

 Michael Kassiou

michael.kassiou@sydney.edu.au

[1]Department of Radiology, Stanford University School of Medicine, Stanford, USA

[2]School of Chemistry, The University of Sydney, Sydney, Australia

[3]Faculty of Medicine and Health Sciences, Macquarie University, Sydney, Australia

[4]Global Health Institute, Ecole Polytechnique Fédérale de Lausanne, Lausanne, Switzerland

[5]Intitute of Chemical Sciences and Engineering, Ecole Polytechnique Fédérale de Lausanne, Lausanne, Switzerland

[6]School of Psychology, The University of Sydney, Sydney, Australia

[7]Faculty of Pharmacy, The University of Sydney, Sydney, Australia

[8]School of Medical Sciences, The University of Auckland, Auckland, New Zealand

[9]Faculty of Health Sciences, The University of Sydney, Sydney, Australia

Abstract RCS-4 (4-methoxyphenyl)-1-yl-(1-pentyl-1*H*-indol-3-yl)methanone) represents the first of several *N*-alkyl-3-methoxybenzoylindoles identified by forensic scientists as synthetic cannabinoid designer drugs. Despite the detection of RCS-4, and several analogues (RCS-2, RCS-3, RCS-2-C4, RCS-3-C4, and RCS-4-C4), in products intended for human consumption, relatively little is known about this class of cannabinoids. The synthesis of all regioisomers of RCS-4 and its C4 homologue is described. This study also systematically explored the structure-activity relationships of this class of synthetic cannabinoids at human CB_1 and CB_2 receptors using an in vitro fluorometric imaging plate reader membrane potential assay. All compounds demonstrated agonist activity at CB_1 (EC_{50} = 54–574 nM) and CB_2 (EC_{50} = 4.5–46 nM) receptors, with the C4 homologues showing a preference for CB_2 receptors (31–42 times). Since most of the analogues (RCS-2, RCS-3, RCS-2-C4, RCS-3-C4 and RCS-4-C4) are not subject to regulation in much of the world, despite their activities towards CB_1 and CB_2 receptors, there is a possibility that these analogues will emerge on the black market.

Keywords synthetic cannabinoid · RCS-4 analogues · RCS-4-C4 · RCS-2-C4 · structure-activity relationship

Introduction

Herbal smoking mixtures adulterated with synthetic cannabinoids (SCs) have been available internationally as unregulated "legal" cannabis alternatives since approximately 2004 [1]. The earliest such product, "Spice", was disingenuously marketed as incense and labeled "not for human consumption", but was later found to contain psychoactive SCs JWH-018 (**1**, Fig. 1) and CP 47,497 (**2**) [2]. Like the principal bioactive component of cannabis, Δ^9-tetrahydrocannabinol (Δ^9-THC, **3**), many SCs exert agonist activities at both cannabinoid receptor subtypes (CB_1 and CB_2 receptors), with psychoactivity attributed to CB_1 activation [3]. Unlike Δ^9-THC, SC intoxication is associated with severe acute toxicity, including myocardial infarction and seizure [4-11].

The European Monitoring Centre for Drugs and Drug Addiction (EMCDDA) reports that 74 new SCs have been identified in marketed products since 2008, with 29 novel SCs formally notified in 2013 alone, making SCs the most rapidly expanding class of "designer drugs" [12]. Although early SCs had been reported by academia or the pharmaceutical industry, many recent examples are unknown in the scientific literature and appear to be the products of clandestine rational design [13], such as *N*-alkylated (methoxybenzoyl)indoles (**4**–**9**). The first reported member of this class, RCS-4 (**9,** also sold online as OBT-199, SR-19, BTM-4, and Eric-4) was identified by Nakajima and colleagues of the Tokyo Metropolitan Institute of Public Health in January 2011 [14], followed by the 2-methoxy regioisomer (RCS-2, **7**) by the same group later that year [15].

RCS-4 has been identified in commercial products seized in the USA [16], Belgium [17], South Korea [18], and New Zealand [19], suggesting widespread use internationally. In 2011, RCS-4 was the third most common substance identified in "herbal highs" products obtained in Poland [20]. A survey of SC products in Germany in 2011 found RCS-4 in a

herbal blend at a concentration of 157 mg/g, one of the highest SC contents of all samples tested in that study [21]. However, various products from Japan contained RCS-4 at concentrations of 18 mg/g and 1.7 mg/g herbal matter, suggesting limited knowledge about the potency of this compound by manufacturers [14]. The *N*-butyl homologue of RCS-4, RCS-4-C4 (**6**), was found in products purchased in New Zealand in July 2011 [19], and the regioisomeric RCS-2-C4 (**4**) was identified in seized products by researchers at the National Forensic Service in South Korea in October 2012 [22]. The same group also found RCS-2 (**7**) and RCS-3 (**8**) in their seizure materials until June 2013 [23]. The structures of the homologues of RCS-4, together with JWH-018, CP 47,497, and Δ^9-THC are shown in Fig. 1.

[INSERT FIGURE 1]

Despite the global availability and popularity of *N*-alkyl-3-(methoxybenzoyl)indole SCs, very little is known of their pharmacology. RCS-4 is the most widely studied member of this class of SCs, and extensive metabolic profiling of RCS-4 has been reported [24-27]. Forensic chemists have also focused on the development of analytical methods for detection and quantification of RCS-4 and its metabolites in human hair [28], urine [29-31], serum [32], and oral fluid [33, 34], with less attention given to RCS-2, and a complete dearth of information regarding the other RCS analogues. Indeed, a method for the detection and quantification of RCS-2, RCS-3, RCS-4, and RCS-4-C4 in human whole blood represents the only report of RCS-3 in the scientific literature [35].

The aim of the present work was to prepare and structurally characterize compounds **4**–**9**, and to determine and compare the functional activity of these novel SCs at cannabinoid receptors in vitro. All compounds were screened against CB_1 and CB_2 receptors in a fluorometric imaging plate reader (FLIPR) membrane potential assay to suggest structure-activity relationships for this class of SCs.

Materials and methods

General chemical synthesis details

All reactions were performed under an atmosphere of nitrogen or argon unless otherwise specified. Toluene was dried over sodium wire and distilled from sodium benzophenone ketyl. Dichloromethane and methanol were distilled from calcium hydride. Anhydrous *N*,*N*-dimethylformamide (DMF) (Sigma-Aldrich, St. Louis, MO, USA) was used as purchased. Commercially available chemicals (Sigma-Aldrich) were used as purchased. Analytical thin layer chromatography (TLC) was performed using Merck aluminum-backed silica gel 60 F254 (0.2 mm) plates (Merck, Darmstadt, Germany) which were visualized using shortwave (254 nm) ultra-violet fluorescence. Flash chromatography was performed using Merck Kieselgel 60 (230–400 mesh) silica gel. Melting points were measured in open capillaries using a Stuart SMP10 melting point apparatus (Bibby Scientific, Staffordshire, UK) and are uncorrected. Nuclear magnetic resonance spectra were recorded at 300 K using either a Bruker AVANCE DRX400 (400.1 MHz) or AVANCE III 500 Ascend (500.1 MHz) spectrometer (Bruker, Bremen, Germany). The data are reported as chemical shift (δ ppm) relative to the residual protonated solvent resonance, relative integral, multiplicity (s = singlet, br s = broad singlet, d = doublet, t = triplet, q = quartet, sep = septet, m = multiplet), coupling constants (*J* Hz) and assignment. Assignment of signals was assisted by correlation spectroscopy (COSY), distortionless enhancement by polarization transfer (DEPT), heteronuclear single quantum coherence (HSQC), and heteronuclear multiple-bond correlation (HMBC) experiments where necessary. Low resolution mass spectra (LRMS) was recorded using electrospray ionization (ESI) recorded on a Finnigan LCQ ion

trap spectrometer (ThermoFisher Scientific, Waltham, MA, USA). Elemental analysis was obtained from the Chemical Analysis Facility in the Department of Chemistry and Biomolecular Sciences, Macquarie University, Australia.

General procedure for 1-alkylation of indole

A cooled (0 ºC) suspension of sodium hydride (60% dispersion in mineral oil, 1.20 g, 30 mmol, 1.5 equiv.) in DMF (35 ml) was treated slowly with a solution of indole (2.34 g, 20.0 mmol) in DMF (5 ml), warmed to ambient temperature and stirred for 10 min. The mixture was cooled to 0 ºC, treated portionwise with the appropriate 1-bromoalkane (21.0 mmol, 1.05 equiv.), warmed to ambient temperature and stirred for 1 h. The reaction was poured portionwise onto ice-water (400 ml) and extracted with ethyl acetate (4 × 50 ml). The combined organic extracts were washed with H_2O (2 × 200 ml), brine (200 ml), dried ($MgSO_4$), and the solvent evaporated under reduced pressure. The crude products were purified using flash chromatography.

1-Butylindole (10)

Indole was treated with 1-bromobutane (2.26 ml) according to the general procedure and the crude material purified by flash chromatography, eluting with hexane (R_f 0.26) to give **10** as a colorless oil (2.90 g, 84%). ^{1}H NMR (500 MHz, $CDCl_3$): δ 7.70 (1H, d, J = 8.0 Hz), 7.41 (1H, d, J = 8.0 Hz), 7.27 (1H, dd, J = 8.8, 8.0 Hz), 7.12-7.09 (2H, m), 6.55 (1H, d, J = 4.0 Hz), 4.16 (2H, t, J = 7.2 Hz), 1.86 (2H, quin., J = 7.6 Hz), 1.41 (2H, quin., J = 7.6 Hz), 1.0 (3H, t, J = 7.6 Hz). All spectroscopic data matched those previously reported [34].

1-Pentylindole (11)

Indole was treated with 1-bromopentane (3.25 ml) according to the general procedure and the crude material purified by flash chromatography, eluting with hexane (R_f 0.32), gave **11** as a pale yellow oil (3.75 g, 80%). ^{1}H NMR (500 MHz, $CDCl_3$): δ 7.64 (1H, d, J = 7.9 Hz), 7.35 (1H, d, J = 8.3 Hz), 7.22-7.19 (1H, m), 7.12-7.09 (2H, m), 6.49 (1H, d, J = 3.1 Hz), 4.12 (2H, t, J = 7.2 Hz), 1.85 (2H, quin., J = 7.3 Hz), 1.40-1.26 (4H, m), 0.90 (3H, t, J = 7.1 Hz). All spectroscopic data matched those previously reported [37].

General procedure for 3-acylation of 1-alkylindoles

A solution of the appropriate carboxylic acid (1.2 mmol, 1.2 equiv.) in dichloromethane (4 ml) was treated with $(COCl)_2$ (205 μl, 2.4 mmol, 2.4 equiv.) followed by DMF (1 drop). After stirring for 1 h, the solution was evaporated in vacuo, and the crude acid chloride was used immediately in the following step.

A cooled (0 °C) solution of appropriate 1-alkylindole (1.0 mmol, 1.0 equiv.) in dichloromethane (3 ml) was treated dropwise with a solution of 1 M Me_2AlCl in hexane (1.5 ml, 1.5 mmol, 1.5 equiv.) and stirred for 30 min. To this solution was added dropwise a solution of the freshly prepared acid chloride in dichloromethane (3 ml), and the reaction stirred for 4 h. The reaction was quenched by dropwise addition to a solution of 1 M aq. HCl (6 ml), the layers separated, and the aqueous phase extracted with dichloromethane (2 × 10 ml). The combined organic layers were washed with sat. aq. $NaHCO_3$ (2 × 10 ml), brine (10 ml), dried ($MgSO_4$), and the solvent evaporated under reduced pressure. The crude products were purified by flash chromatography.

(1-Butyl-1*H*-indol-3-yl)(2-methoxyphenyl)methanone (4)

Treating **10** (187 mg, 1.0 mmol) with 2-methoxybenzoic acid (183 mg, 1.2 mmol) according to the general procedure gave, following purification by flash chromatography (hexane/ethyl acetate, 80:20, R_f 0.28), **4** (215 mg, 70%) as a white crystalline solid. Recrystallization from isopropanol-H_2O yielded colorless needles. m.p. (isopropanol-H_2O) 97–99 °C; ^{1}H NMR (500 MHz, $CDCl_3$): δ 8.37-8.35 (1H, m), 7.45-7.39 (3H, m), 7.37-7.35 (1H, m), 7.33-7.29 (2H, m), 7.05-7.01 (2H, m), 4.10 (2H, t, J = 7.5 Hz), 3.79 (3H, s), 1.83 (2H, quin., J = 7.5 Hz), 1.38-1.31 (2H, m), 0.94 (3H, t, J = 7.5 Hz); ^{13}C NMR (125 MHz, $CDCl_3$): δ 190.2 (CO), 157.0 (quat.), 137.9, 137.1 (quat.), 131.4 (quat.), 130.9, 129.1, 127.0 (quat.), 123.5, 123.0, 122.8, 120.4, 117.3 (quat.), 111.7, 110.0, 55.9 (OCH_3), 47.0 (CH_2), 32.0 (CH_2), 20.2 (CH_2), 13.7 (CH_3); LRMS (+ESI) *m/z* 636.80 ($[2M + Na]^+$, 100%), 614.27 ($[2M]^+$, 23%), 330.00 ($[M + Na]^+$, 19%), 308.00 ($[M + H]^+$, 58%); Anal. ($C_{20}H_{21}NO_2$) calcd: C 78.15, H 6.89, N 4.56; found: C 78.10, H 6.99, N 4.71.

(1-Butyl-1*H*-indol-3-yl)(3-methoxyphenyl)methanone (5)

Treating **10** (187 mg, 1.0 mmol) with 3-methoxybenzoic acid (183 mg, 1.2 mmol) according to the general procedure gave, following purification by flash chromatography (hexane/ethyl acetate, 80:20, R_f 0.34), **5** (207 mg, 67%) as a pale yellow oil. ^{1}H NMR (500 MHz, $CDCl_3$): δ 8.44-8.42 (1H, m), 7.59 (1H, s), 7.40-7.33 (6H, m), 7.11-7.08 (1H, m), 4.16 (2H, t, J = 7.5 Hz), 3.87 (3H, s), 1.86 (2H, quin., J = 7.5 Hz), 1.41-1.33 (2H, m), 0.95 (3H, t, J = 7.5 Hz); ^{13}C NMR (125 MHz, $CDCl_3$): δ 190.7 (CO), 159.7 (quat.), 142.5 (quat.), 137.1, 137.0 (quat.), 129.4, 127.5 (quat.), 123.7, 123.0, 122.8, 121.4, 117.5, 115.7 (quat.), 113.6, 110.0, 55.6

(OCH_3), 47.1 (CH_2), 32.1 (CH_2), 20.3 (CH_2), 13.8 (CH_3); LRMS (+ESI) *m*/*z* 636.80 ([2M + Na]$^+$, 100%), 614.47 ([2M]$^+$, 28%), 330.00 ([M + Na]$^+$, 15%), 308.00 ([M + H]$^+$, 78%).

(1-Butyl-1*H*-indol-3-yl)(4-methoxyphenyl)methanone (6)

Treating **10** (187 mg, 1.0 mmol) with 4-methoxybenzoic acid (183 mg, 1.2 mmol) according to the general procedure gave, following purification by flash chromatography (hexane/ethyl acetate, 80:20, R_f 0.36), **6** (241 mg, 78%) as a white crystalline solid. Recrystallization from isopropanol-H_2O yielded colorless needles. m.p. (isopropanol-H_2O) 100–102 °C; ^{1}H NMR (500 MHz, $CDCl_3$): δ 8.37-8.36 (1H, m), 7.85 (2H, d., J = 8.8 Hz), 7.60 (1H, s), 7.41-7.39 (1H, m), 7.35-7.30 (2H, m), 7.00 (2H, d., J = 8.8 Hz), 4.17 (2H, t, J = 7.5 Hz), 3.90 (3H, s), 1.87 (2H, quin., J = 7.5 Hz), 1.41-1.34 (2H, m), 0.96 (3H, t, J = 7.5 Hz); ^{13}C NMR (125 MHz, $CDCl_3$): δ 189.9 (CO), 162.3 (quat.), 136.9 (CH), 136.2 (quat.), 133.7 (quat.), 131.0 (CH), 127.6 (quat.), 123.4 (CH), 122.9 (CH), 122.5 (CH), 115.8 (quat.), 113.7 (CH), 109.9 (CH), 55.6 (OCH_3), 47.0 (NCH_2), 32.1 (CH_2), 20.2 (CH_2), 13.7 (CH_3); LRMS (+ESI) *m*/*z* 636.80 ([2M + Na]$^+$, 100%), 614.47 ([2M]$^+$, 63%), 329.93 ([M + Na]$^+$, 27%), 308.07 ([M + H]$^+$, 95%); Anal. ($C_{20}H_{21}NO_2$) calcd: C 78.15, H 6.89, N 4.56; found: C 77.95, H 6.91, N 4.68.

(1-Pentyl-1*H*-indol-3-yl)(2-methoxyphenyl)methanone (7)

Treating **11** (187 mg, 1.0 mmol) with 2-methoxybenzoic acid (183 mg, 1.2 mmol) according to the general procedure gave, following purification by flash chromatography (hexane/ethyl acetate, 80:20, R_f 0.25), **7** (266 mg, 83%) as a white crystalline solid. Recrystallization from isopropanol-H_2O yielded colorless needles. m.p. (isopropanol-H_2O) 77–78 °C; ^{1}H NMR (500

MHz, $CDCl_3$): δ 8.39-8.38 (1H, m), 7.45-7.29 (6H, m), 7.05-7.01 (2H, m), 4.08 (2H, t, J = 7.5 Hz), 3.79 (3H, s), 1.84 (2H, quin., J = 7.5 Hz), 1.36-1.28 (4H, m), 0.89 (3H, t, J = 7.5 Hz); ^{13}C NMR (125 MHz, $CDCl_3$): δ 190.2 (CO), 156.9 (quat.), 137.8, 137.0 (quat.), 131.4 (quat.), 130.8, 129.0, 126.9 (quat.), 123.4, 122.9, 122.7, 120.3, 117.2 (quat.), 111.7, 109.9, 55.8 (OCH_3), 47.2 (CH_2), 29.6 (CH_2), 29.0 (CH_2), 22.3 (CH_2), 14.0 (CH_3); LRMS (+ESI) m/z 664.80 ($[2M + Na]^+$, 100%), 642.20 ($[2M]^+$, 30%), 344.00 ($[M + Na]^+$, 17%), 322.07 ($[M + H]^+$, 66%); Anal. ($C_{21}H_{23}NO_2$) calcd: C 78.47, H 7.21, N 4.36; found: C 78.57, H 7.23, N 4.45.

(1-Pentyl-1*H*-indol-3-yl)(3-methoxyphenyl)methanone (8)

Treating **11** (187 mg, 1.0 mmol) with 3-methoxybenzoic acid (183 mg, 1.2 mmol) according to the general procedure gave, following purification by flash chromatography (hexane/ethyl acetate, 80:20, R_f 0.38), **8** (241 mg, 75%) as a pale yellow oil. ^{1}H NMR (500 MHz, $CDCl_3$): δ 8.44-8.42 (1H, m), 7.60 (1H, s), 7.40-7.32 (6H, m), 7.12-7.09 (1H, m), 4.15 (2H, t, J = 7.5 Hz), 3.87 (3H, s), 1.88 (2H, quin., J = 7.5 Hz), 1.37-1.31 (4H, m), 0.89 (3H, t, J = 7.5 Hz); ^{13}C NMR (125 MHz, $CDCl_3$): δ 190.7 (CO), 159.7 (quat.), 142.5 (quat.), 137.1, 137.0 (quat.), 129.4, 127.5 (quat.), 123.7, 123.0, 122.8, 121.4, 117.5, 115.6 (quat.), 113.6, 110.0, 55.6 (OCH_3), 47.3 (CH_2), 29.7 (CH_2), 29.1 (CH_2), 22.4 (CH_2), 14.0 (CH_3); LRMS (+ESI) m/z 664.73 ($[2M + Na]^+$, 90%), 642.32 ($[2M]^+$, 37%), 343.93 ($[M + Na]^+$, 21%), 322.00 ($[M + H]^+$, 100%).

(1-Pentyl-1*H*-indol-3-yl)(4-methoxyphenyl)methanone (9)

Treating **11** (187 mg, 1.0 mmol) with 4-methoxybenzoic acid (183 mg, 1.2 mmol) according to the general procedure gave, following purification by flash chromatography (hexane/ethyl acetate, 80:20, R_f 0. 36), **9** (265 mg, 82%) as a white crystalline solid. Recrystallization from isopropanol-H_2O yielded colorless needles. m.p. (isopropanol-H_2O) 116–118 °C; ^{1}H NMR (500 MHz, $CDCl_3$): δ 8.39-8.37 (1H, m), 7.85 (2H, d., J = 9.0 Hz), 7.58 (1H, s), 7.40-7.38 (1H, m), 7.34-7.31 (2H, m), 6.99 (2H, d., J = 9.0 Hz), 4.15 (2H, t, J = 7.5 Hz), 3.89 (3H, s), 1.88 (2H, quin., J = 7.5 Hz), 1.36-1.31 (4H, m), 0.90 (3H, t, J = 7.5 Hz); ^{13}C NMR (125 MHz, $CDCl_3$): δ 189.9 (CO), 162.3 (quat.), 136.9 (quat.), 136.3, 133.7 (quat.), 131.0, 127.6 (quat.), 123.4, 122.9, 122.5, 115.7 (quat.), 113.6, 109.9, 55.5 (OCH_3), 47.2 (CH_2), 29.7 (CH_2), 29.1 (CH_2), 22.3 (CH_2), 14.0 (CH_3); LRMS (+ESI) *m*/*z* 664.67 ($[2M + Na]^+$, 76%), 642.53 ($[2M]^+$, 88%), 343.87 ($[M + Na]^+$, 24%), 321.93 ($[M + H]^+$, 100%); Anal. ($C_{21}H_{23}NO_2$) calcd: C 78.47, H 7.21, N 4.36; found: C 78.54, H 7.31, N 4.49.

Ultraviolet absorption spectroscopy

Ultraviolet (UV) absorption spectroscopy was performed using a Cary 60 UV-Vis Spectrophotomer (Agilent Technologies, Santa Clara, CA, USA). UV absorbance of solutions of **4**–**9** in methanol (0.001% w/v) in quartz cuvette was recorded over 200–400 nm.

Gas chromatography–mass spectrometry

All SCs were analyzed by gas chromatography–mass spectrometry (GC–MS) using a ThermoQuest Trace gas chromatograph with Finnigan Polaris Q ion trap mass spectrometer (ThermoQuest, Madison, CT, USA) in positive ion electron ionization (EI) mode and Phenomex ZB Wax column (30 m × 0.25 mm internal diameter × 0.25 μm film thickness;

Phenomenex, Torrance, CA, USA) with helium gas as carrier at 1.3 ml/min. The conditions were: electron energy, 70 eV; injector temperature, 250 °C; injection, split mode (10:1); injection volume, 1 µl; oven temperature program , 40 °C (2 min-hold) and increase at a rate of 20 °C/min to 270 °C (20 min-hold for **4** and **7**, 40 min hold for **5**, **6**, **8**, and **9**); transfer line temperature, 250 °C; scan range, *m/z* 46–650 (5 min solvent delay).

X-Ray data collection

Solid **9** was recrystallized from isopropanol-H_2O to give colorless needle crystals by slow evaporation at ambient temperature. The single-crystal X-ray diffraction experiments were carried out at the Faculty of Pharmacy, University of Sydney using a Bruker APEX-II CCD-based diffractometer with an X-ray wavelength of 0.71073 Å (Mo Kα) and at an experimental temperature of 150 K. The single crystal of **9** was mounted on the tip of a thin glass fiber with a minimum amount of Paratone N oil, which acted as both an adhesive and a cryoprotectant, and inserted in the cold N_2 stream of an Oxford Cryosystem COBRA cooler (Oxford Cryosystems, Oxford, UK). X-ray diffraction data were collected using 0.3°$\Delta\omega$-scans, maintaining the crystal-to-detector distance at 6.0 cm. A total of 1664 frames were collected. The diffraction data were integrated using SAINT+ [38], which included corrections for Lorentz, polarization and absorption effects. Unit cell parameters for **9** at 150 K were refined from 999 reflections.

The structure was solved using Direct Methods (SHELX-S) [39], and refined using full-matrix least-squares (SHELXL) [39]. All non-hydrogen atoms were treated as anisotropic, while hydrogen atoms were placed in idealized positions, with U_{eq} set at 1.5 times that of the parent atom.

Empirical formula	$C_{21}H_{23}NO_2$
Formula weight	321.40
Temperature	150.2 K
Crystal system, space group	monoclinic, $P2_1/c$
Unit cell dimensions	a = 13.020 Å, α = 90°
	b = 9.312 Å, β = 101.78°
	c = 14.506 Å, γ = 90°
Z	4
Goodness-of-fit on F^2	1.036
Final R indices [I>2σ(I)]	R_1 = 0.0382, wR_2 = 0.0941
R indices (all data)	R_1 = 0.0510, wR_2 = 0.1013

In vitro pharmacological assessment of 4−9

Mouse AtT-20 neuroblastoma cells stably transfected with human CB_1 or human CB_2 have been previously described [40, 41] and were cultured in Dulbecco's modified Eagle's medium (DMEM) containing 10% fetal bovine serum (FBS), 100 U penicillin/streptomycin, and 300 μg/ml G418. Cells were passaged at 80% confluency as required. Cells for assays were grown in 75 cm^2 flasks and used at 90% confluence. The day before the assay cells were detached from the flask with trypsin/EDTA (Sigma-Aldrich) and resuspended in 10 ml of Leibovitz's L-15 media supplemented with 1% FBS, 100 U penicillin/streptomycin and 15 mM glucose (membrane potential assay and Ca5 calcium assay). The cells were plated in volume of 90 μl in black walled, clear bottomed 96-well microplates (Corning, Oneonta, NY, USA) which had been precoated with poly-L-lysine (Sigma-Aldrich). Cells were incubated overnight at 37 °C in ambient CO_2.

Membrane potential was measured using a FLIPR membrane potential assay kit (blue) from Molecular Devices (Sunnyvale, CA, USA), as described previously [42]. The dye was reconstituted with assay buffer of composition (mM): NaCl 145, HEPES 22, Na_2HPO_4 0.338, $NaHCO_3$ 4.17, KH_2PO_4 0.441, $MgSO_4$ 0.407, $MgCl_2$ 0.493, $CaCl_2$ 1.26, glucose 5.56 (pH 7.4, osmolarity 315 ± 5). Prior to the assay, cells were loaded with 90 μl/well of the dye solution without removal of the L-15, giving an initial assay volume of 180 μl/well. Plates were then incubated at 37 °C at ambient CO_2 for 45 min. Fluorescence was measured using a FlexStation 3 (Molecular Devices) microplate reader with cells excited at a wavelength of 530 nm and emission measured at 565 nm. Baseline readings were taken every 2 s for at least 2 min, at which time either drug or vehicle was added in a volume of 20 μl. The background fluorescence of cells without dye or dye without cells was negligible. Changes in fluorescence were expressed as a percentage of baseline fluorescence after subtraction of the changes produced by vehicle addition, which was less than 2% for drugs dissolved in assay buffer or DMSO. The final concentration of dimethyl sulfoxide was not more than 0.1%.

Data were analyzed with PRISM (GraphPad Software Inc., San Diego, CA), using four-parameter nonlinear regression to fit concentration-response curves. In all plates, a maximally effective concentration of WIN 55,212-2 (Cayman Chemical, Ann Arbor, MI, USA) was added to allow for normalization between assays.

Results and discussion

The synthesis of **4**–**9** is shown in Scheme 1. Indole was alkylated with either 1-bromobutane or 1-bromopentane to quantitatively afford the desired *N*-alkylindoles **10** and **11** respectively. Subjecting *N*-alkylindoles **10** and **11** to acylation under Okauchi conditions [43] with freshly

prepared 2-, 3-, or 4-methoxybenzoyl chloride gave the desired products in excellent yields after chromatographic purification.

[INSERT FIGURE 2]

RCS-2-C4, RCS-4-C4, RCS-2 and RCS-4 could be recrystallized from isopropanol-water to afford highly crystalline material, whereas RCS-3-C4 and RCS-3 were obtained as oils. Attempts to crystallize RCS-3-C4 and RCS-3 using various high vacuum and low temperature techniques were unsuccessful. A highly prismatic single crystal of RCS-4 was selected from the bulk mixture, allowing the generation of the first X-ray crystal structure for this class of SCs. An Oak Ridge Thermal-Ellipsoid Plot Program (ORTEP) representation of RCS-4 is shown in Fig. 3. All bond lengths and angles were as expected (full details of X-ray data collection and tables of bond lengths and angles available in the Supporting Information), with the pentyl chain in a fully extended conformation and the methoxybenzene group out-of-plane with the indole ring.

[INSERT FIGURE 3]

All SCs were analyzed using GC−MS, and total ion current chromatograms (TICs) and EI mass spectra for *N*-butyl-3-(methoxybenzoyl)indoles (**4**−**6**) and *N*-pentyl analogues (**7**−**9**) are shown in Fig. 4. All *N*-butyl-3-(methoxybenzoyl)indoles demonstrated molecular ion peaks at *m/z* 307, while their *N*-pentyl analogues showed molecular ion peaks at *m/z* 321. The major fragmentation ions for **4**−**6** were *m/z* 264 and *m/z* 200. The former arises from cleavage of the butyl chain between the two carbon atoms most proximal to the indole nitrogen (C1–C2), while the latter can be attributed to loss of the methoxyphenyl ring. Other fragmentation ions observed were *m/z* 172 and 135, each representing the fragments remaining after cleavage of the methoxybenzoyl unit. For **4**, *m/z* 144 was prominent, and represents a protonated species featuring loss of the methoxyphenyl ring and pentyl chain.

The peak at *m/z* 290 likely results from the loss of a hydroxyl group, although the mechanism is unclear.

The fragmentation patterns for **7**–**9** were analogous, with fragmentation ion *m/z* 264 appearing due to corresponding fragmentation of the pentyl chain C1–C2 bond, and *m/z* 214 consistent with loss of the methoxyphenyl ring. Similarly, cleavage of the whole methoxybenzoyl group of **7**–**9** gave *m/z* 186 and *m/z* 135. As for **4**, *m/z* 144 was observed for **7**, as well as a peak at *m/z* 290, corresponding to the loss of 17 mass units.

[INSERT FIGURE 4]

The ultraviolet absorption spectra of **4**–**9** are shown in Fig. 5, and peak absorbances are similar for each corresponding *N*-butyl and *N*-pentyl regioisomer, as expected.

[INSERT FIGURE 5]

The cannabinoid activities of RCS analogues **4**–**9** at CB_1 and CB_2 receptors, together with that of the phytocannabinoid Δ^9-THC, a partial agonist at CB_1 and CB_2, are shown in Table 1. Murine AtT-20 neuroblastoma cells were stably transfected with human CB_1 or CB_2 receptors, and activities of Δ^9-THC and **4**–**9** were evaluated using a FLIPR membrane potential assay whereby endogenously expressed G protein-gated inwardly rectifying K^+ channels (GIRKs) are activated by agonists at the coexpressed CB_1 or CB_2 receptors.[42, 44] The maximum effects of **4**–**9** were compared to the high efficacy CB_1/CB_2 receptor full agonist WIN 55,212-2, which produced a maximal decrease in fluorescence, corresponding to cellular hyperpolarization, of 29 ± 2% in AtT-20-CB_1 cells and 31 ± 3% in AtT-20-CB_2 cells. None of the compounds produced a significant change in the membrane potential of wild type AtT-20 cells, which did not express CB_1 or CB_2 receptors.

[INSERT TABLE 1]

All RCS analogues activated CB_1 and CB_2 receptors. RCS-2 (54 nM) had about 5-fold greater potency than Δ^9-THC (250 nM) for CB_1 receptor-mediated activation of GIRK, the

other compounds had a similar potency to Δ^9-THC (Table 1). Δ^9-THC is a low efficacy CB_2 agonist, and in the assay of GIRK activation in AtT20-CB_2, its effects at 10 μM were only 13% of that of WIN 55,212-2.

WIN 55,212-2 was more potent at stimulating a cellular hyperpolarization in AtT-20-CB_2 cells than AtT-20-CB_1 cells, displaying about 5-fold CB_2 preference. The *N*-pentyl indoles RCS-2, RCS-3, and RCS-4 had a similar maximal effect to WIN 55,212-2 at both CB_1 and CB_2 receptors, and also showed a similar CB_2 preference (Table 1 and Fig 6). This indicates that these drugs are also high efficacy agonists.

The *N*-butyl indoles RCS-2-C4, RCS-3-C4, and RCS-4-C4 had generally similar efficacies to WIN 55,212-2 at CB_2 receptors, but were significantly more potent than WIN 55,212-2; and their CB_2 selectivity was greater than 30-fold (Table 1). Interestingly, their CB_1 efficacy fell between that of WIN 55,212-2 and Δ^9-THC, indicating a relatively moderate CB_1 efficacy (Fig. 6).

The 2-methoxy-substituted indoles (RCS-2, RCS-2-C4) were both relatively more potent than the corresponding 3-methoxy regioisomers, while the 4-methoxy compounds were the least potent at both CB_1 and CB_2 receptors (Table 1). It should be noted that while the potency of any drug effect depends on the number of receptors expressed in the system under study, and we have not directly measured the number of receptors in our AtT-20-CB_1 and -CB_2 cells at the time of these assays; WIN 55,212-2 is recognized as having a higher affinity for CB_2 receptors than CB_1 receptors in binding assays,[45, 46] so it likely that that CB_2 preference of the RCS analogues is genuine, and not an artifact of our expression systems.

[INSERT FIGURE 6]

Conclusions

This study represents the first pharmacological characterization of the designer drug RCS-4, as well as several of its regioisomers and *N*-butyl analogues of forensic interest. A general synthetic route to RCS-4 and its analogues was demonstrated, and this may prove useful for the preparation of other *N*-alkyl-3-acylindoles of relevance to forensic toxicologists and cannabinoid researchers. RCS-4 and its analogues were tested as agonists of CB_1 and CB_2 receptors in a FLIPR membrane potential assay. Preliminary structure-activity relationships suggest that an *N*-butyl substituent on the indole ring primarily confers functional selectivity for CB_2 receptors, while an N-pentyl group at the same position increases potency at CB_1 receptors, leading to a net reduction in CB_2 selectivity. The position of the methoxy group on the benzoyl ring appeared to have little effect on activity, but it should be noted that the 2-position conferred the greatest potency at CB_1 and CB_2 in both the *N*-butyl and *N*-pentyl series. This study demonstrates that RCS-4, as well as its regioisomers and their C4 homologues, are all actively cannabimimetic in vitro. Since several RCS-4 regioisomers and their C4 homologues are not subject to regulation in much of the world, there is a possibility that these analogues will emerge on the black market.

Acknowledgements Work was supported in part by the European Union's Seventh Framework Programme [FP7/2007-2013] INMiND (Grant agreement No. HEALTH-F2-2011-278850). MC supported by NHMRC Project Grant 1002680, JS by an iMQRES Postgraduate Scholarship from Macquarie University.

Conflict of interest There are no financial or other relations that could lead to a conflict of interest.

Ethical approval This article does not contain any studies with human participants or animals performed by any of the authors.

References

1. Dresen S, Ferreiros N, Putz M, Westphal F, Zimmermann R, Auwärter V (2010) Monitoring of herbal mixtures potentially containing synthetic cannabinoids as psychoactive compounds. J Mass Spectrom 45:1186-1194
2. Auwärter V, Dresen S, Weinmann W, Muller M, Putz M, Ferreiros N (2009) 'Spice' and other herbal blends: harmless incense or cannabinoid designer drugs? J Mass Spectrom 44:832-837
3. Pertwee RG, Howlett AC, Abood ME, Alexander SPH, Di Marzo V, Elphick MR, Greasley PJ, Hansen HS, Kunos G, Mackie K, Mechoulam R, Ross A (2010) International Union of Basic and Clinical Pharmacology. LXXIX. Cannabinoid receptors and their ligands: beyond CB_1 and CB_2. Pharmacol Rev 62:588-631
4. Seely KA, Lapoint J, Moran JH, Fattore L (2012) Spice drugs are more than harmless herbal blends: a review of the pharmacology and toxicology of synthetic cannabinoids. Prog Neuropsychopharmacol Biol Psychiatry 39:234-243
5. Mir A, Obafemi A, Young A, Kane C (2011) Myocardial infarction associated with use of the synthetic cannabinoid K2. Pediatrics 128:e1622 -e1627
6. Lapoint J, James LP, Moran CL, Nelson LS, Hoffman RS, Moran JH (2011) Severe toxicity following synthetic cannabinoid ingestion. Clin Toxicol 49:760-764
7. Simmons J, Cookman L, Kang C, Skinner C (2011) Three cases of "spice" exposure. Clin Toxicol 49:431-433
8. Schneir AB, Cullen J, Ly BT (2011) “Spice” girls: Synthetic cannabinoid intoxication. J Emerg Med 40:296-299
9. Schneir A, Baumbacher T (2012) Convulsions associated with the use of a synthetic cannabinoid product. J Med Toxicol 8:62-64

10. Harris CR, Brown A (2013) Synthetic cannabinoid intoxication: a case series and review. J Emerg Med 44:360-366

11. Uchiyama N, Shimokawa Y, Kawamura M, Kikura-Hanajiri R, Hakamatsuka T (2014) Chemical analysis of a benzofuran derivative, 2-(2-ethylaminopropyl)benzofuran (2-EAPB), eight synthetic cannabinoids, five cathinone derivatives, and five other designer drugs newly detected in illegal products. Clin Toxicol 32:266-281

12. European Monitoring Centre for Drugs and Drug Addictions (2014) European Drug Report 2014: trends and developments. doi:10.2810/32306

13. Wilkinson SM, Banister SD, Kassiou M (2015) Bioisosteric fluorine in the clandestine design of synthetic cannabinoids. Aust J Chem 68:4-8

14. Nakajima J, Takahashi M, Seto T, Kanai C, Suzuki J, Yoshida M, Hamano T (2011) Identification and quantitation of two benzoylindoles AM-694 and (4-methoxyphenyl)(1-pentyl-1*H*-indol-3-yl)methanone, and three cannabimimetic naphthoylindoles JWH-210, JWH-122, and JWH-019 as adulterants in illegal products obtained via the internet. Forensic Toxicol 29:95-110

15. Nakajima J, Takahashi M, Nonaka R, Seto T, Suzuki J, Yoshida M, Kanai C, Hamano T (2011) Identification and quantitation of a benzoylindole (2-methoxyphenyl)(1-pentyl-1*H*-indol-3-yl)methanone and a naphthoylindole 1-(5-fluoropentyl-1*H*-indol-3-yl)-(naphthalene-1-yl)methanone (AM-2201) found in illegal products obtained via the Internet and their cannabimimetic effects evaluated by in vitro [^{35}S]GTPγS binding assays. Forensic Toxicol 29:132-141

16. Logan BK, Reinhold LE, Xu A, Diamond FX (2012) Identification of synthetic cannabinoids in herbal incense blends in the United States. J Forensic Sci 57:1168-1180

17. Denooz R, Vanheugen JC, Frederich M, de Tullio P, Charlier C (2013) Identification and structural elucidation of four cannabimimetic compounds (RCS-4, AM-2201, JWH-203 and JWH-210) in seized products. J Anal Toxicol 37:56-63

18. Choi H, Heo S, Choe S, Yang W, Park Y, Kim E, Chung H, Lee J (2013) Simultaneous analysis of synthetic cannabinoids in the materials seized during drug trafficking using GC-MS. Anal Bioanal Chem 405:3937-3944

19. Couch RAF, Madhavaram H (2012) Phenazepam and cannabinomimetics sold as herbal highs in New Zealand. Drug Test Anal 4:409-414

20. Zuba D, Byrska B (2013) Analysis of the prevalence and coexistence of synthetic cannabinoids in "herbal high" products in Poland. Forensic Toxicol 31:21-30

21. Simolka K, Lindigkeit R, Schiebel H-M, Papke U, Ernst L, Beuerle T (2012) Analysis of synthetic cannabinoids in "spice-like" herbal highs: snapshot of the German market in summer 2011. Anal Bioanal Chem 404:157-171

22. Park Y, Lee C, Lee H, Pyo J, Jo J, Lee J, Choi H, Kim S, Hong R, Park Y, Hwang B, Choe S, Jung J (2013) Identification of a new synthetic cannabinoid in a herbal mixture: 1-butyl-3-(2-methoxybenzoyl)indole. Forensic Toxicol 31:187-196

23. Chung H, Choi H, Heo S, Kim E, Lee J (2014) Synthetic cannabinoids abused in South Korea: drug identifications by the National Forensic Service from 2009 to June 2013. Forensic Toxicol 32:82-88

24. Hutter M, Broecker S, Kneisel S, Auwärter V (2012) Identification of the major urinary metabolites in man of seven synthetic cannabinoids of the aminoalkylindole type present as adulterants in 'herbal mixtures' using LC-MS/MS techniques. J Mass Spectrom 47:54-65

25. Kavanagh P, Grigoryev A, Melnik A, Simonov A (2012) The identification of the urinary metabolites of 3-(4-methoxybenzoyl)-1-pentylindole (RCS-4), a novel

cannabimimetic, by gas chromatography–mass spectrometry. J Anal Toxicol 36:303-311

26. Gandhi AS, Zhu M, Pang S, Wohlfarth A, Scheidweiler KB, Huestis MA (2014) Metabolite profiling of RCS-4, a novel synthetic cannabinoid designer drug, using human hepatocyte metabolism and TOF-MS. Bioanalysis 6:1471-1485

27. Scheidweiler KB, Huestis MA (2014) Simultaneous quantification of 20 synthetic cannabinoids and 21 metabolites, and semi-quantification of 12 alkyl hydroxy metabolites in human urine by liquid chromatography-tandem mass spectrometry. J Chromatogr A 1327:105-117

28. Hutter M, Kneisel S, Auwärter V, Neukamm MA (2012) Determination of 22 synthetic cannabinoids in human hair by liquid chromatography-tandem mass spectrometry. J Chromatogr B 903:95-101

29. Sundstroem M, Pelander A, Angerer V, Hutter M, Kneisel S, Ojanperae I (2013) A high-sensitivity ultra-high performance liquid chromatography/high-resolution time-of-flight mass spectrometry (UHPLC-HR-TOFMS) method for screening synthetic cannabinoids and other drugs of abuse in urine. Anal Bioanal Chem 405:8463-8474

30. Wohlfarth A, Scheidweiler KB, Chen X, Liu H-f, Huestis MA (2013) Qualitative confirmation of 9 synthetic cannabinoids and 20 metabolites in human urine using LC-MS/MS and library search. Anal Chem 85:3730-3738

31. Kronstrand R, Brinkhagen L, Birath-Karlsson C, Roman M, Josefsson M (2014) LC-QTOF-MS as a superior strategy to immunoassay for the comprehensive analysis of synthetic cannabinoids in urine. Anal Bioanal Chem 406:3599-3609

32. Kneisel S, Auwärter V (2012) Analysis of 30 synthetic cannabinoids in serum by liquid chromatography-electrospray ionization tandem mass spectrometry after liquid-liquid extraction. J Mass Spectrom 47:825-835

33. Kneisel S, Speck M, Moosmann B, Corneillie TM, Butlin NG, Auwärter V (2013) LC/ESI-MS/MS method for quantification of 28 synthetic cannabinoids in neat oral fluid and its application to preliminary studies on their detection windows. Anal Bioanal Chem 405:4691-4706

34. Kneisel S, Auwärter V, Kempf J (2013) Analysis of 30 synthetic cannabinoids in oral fluid using liquid chromatography-electrospray ionization tandem mass spectrometry. Drug Test Anal 5:657-669

35. Ammann J, McLaren JM, Gerostamoulos D, Beyer J (2012) Detection and quantification of new designer drugs in human blood: Part 1 - Synthetic cannabinoids. J Anal Toxicol 36:372-380

36. Ito Y, Kobayashi K, Seko N, Saegusa T (1984) Indole syntheses utilizing o-methylphenyl isocyanides. Bull Chem Soc Jpn 57:73-84

37. Blaazer AR, Lange JH, van der Neut MA, Mulder A, den Boon FS, Werkman TR, Kruse CG, Wadman WJ (2011) Novel indole and azaindole (pyrrolopyridine) cannabinoid (CB) receptor agonists: design, synthesis, structure-activity relationships, physicochemical properties and biological activity. Eur J Med Chem 46:5086-5098

38. Bruker (2011) Apex2 suite of programs. Bruker AXS Inc., Madison, Wisconsin, USA

39. Sheldrick GM (2008) A short history of SHELX. Acta Crystallogr A 64:112-122

40. Banister SD, Wilkinson SM, Longworth M, Stuart J, Apetz N, English K, Brooker L, Goebel C, Hibbs DE, Glass M, Connor M, McGregor IS, Kassiou M (2013) The synthesis and pharmacological evaluation of adamantane-derived indoles: cannabimimetic drugs of abuse. ACS Chem Neurosci 4:1081-1092

41. Banister SD, Stuart J, Kevin RC, Edington A, Longworth M, Wilkinson SM, Beinat C, Buchanan AS, Hibbs DE, Glass M, Connor M, McGregor IS, Kassiou M (2015) The effects of bioisosteric fluorine in synthetic cannabinoid designer drugs JWH-018,

AM-2201, UR-144, XLR-11, PB-22, 5F-PB-22, APICA, and STS-135. ACS Chem Neurosci. doi: 10.1021/acschemneuro.5b00107

42. Knapman A, Santiago M, Du YP, Bennallack PR, Christie MJ, Connor M (2013) A continuous, fluorescence-based assay of μ-opioid receptor activation in AtT-20 cells. J Biomol Screen 18:269-276

43. Okauchi T, Itonaga M, Minami T, Owa T, Kitoh K, Yoshino H (2000) A general method for acylation of indoles at the 3-position with acyl chlorides in the presence of dialkylaluminum chloride. Org Lett 2:1485-1487

44. Grimsey NL, Graham ES, Dragunow M, Glass M (2010) Cannabinoid Receptor 1 trafficking and the role of the intracellular pool: implications for therapeutics. Biochem Pharmacol 80:1050-1062

45. Frost JM, Dart MJ, Tietje KR, Garrison TR, Grayson GK, Daza AV, El-Kouhen OF, Miller LN, Li L, Yao BB, Hsieh GC, Pai M, Zhu CZ, Chandran P, Meyer MD (2008) Indol-3-yl-tetramethylcyclopropyl ketones: effects of indole ring substitution on CB_2 cannabinoid receptor activity. J Med Chem 51:1904-1912

46. Frost JM, Dart MJ, Tietje KR, Garrison TR, Grayson GK, Daza AV, El-Kouhen OF, Yao BB, Hsieh GC, Pai M, Zhu CZ, Chandran P, Meyer MD (2010) Indol-3-ylcycloalkyl ketones: effects of N1 substituted indole side chain variations on CB_2 cannabinoid receptor activity. J Med Chem 53:295-315

Figure legends

Fig. 1. Selected natural and synthetic cannabinoids

Fig. 2. Synthesis of cannabinoids **4**–**9**. Reagents and conditions: (**a**) NaH, $Br(CH_2)_4R^1$, *N*,*N*-dimethylformamide, 0 °C–rt, 1 h, 80–84%; (**b**) Me_2AlCl, $R^2PhC(O)Cl$, dichloromethane, 0 °C, 2 h, 67–83%

Fig. 3. An Oak Ridge Thermal-Ellipsoid Plot Program diagram of the crystal structure of **9** with thermal ellipsoids at the 50% probability level

Fig. 4. Gas chromatography–mass spectrometry analyses showing total ion current chromatograms (left) and electron ionization mass spectra (right), respectively, for (**a**) **4**, (**b**) **5**, (**c**) **6**, (**d**) **7**, (**e**) **8**, and (**f**) **9**. Proposed fragmentation ions are superimposed

Fig. 5. Ultraviolet absorption spectra of (**a**) **4**, (**b**) **5**, (**c**) **6**, (**d**) **7**, (**e**) **8**, and (**f**) **9**.

Fig. 6. Hyperpolarization of CB_1 and CB_2 receptors induced by (**a**) RCS-2-C4 (**4**), RCS-3-C4 (**5**), and RCS-4-C4 (**6**) and (**b**) RCS-2 (**7**), RCS-3 (**8**), and RCS-4 (**9**) as a proportion of that produced by 1 μM WIN 55,212-2. Membrane potential was measured using a fluorescent dye, as outlined in the text. Each point represents the mean ± standard error of the mean of at least five independent determinations, each performed in duplicate. Data was fitted with a 4 parameter logistic equation in GraphPad Prism

Table 1 Functional activities of Δ^9-THC, WIN 55,212-2, and **4–9** at human CB_1 and human CB_2 receptors

Compound	hCB_1		hCB_2		CB_2 selectivity[a]
	pEC_{50} ± SEM (EC_{50}, nM)	Max ± SEM (% WIN 55,212-2)	pEC_{50} ± SEM (EC_{50}, nM)	Max ± SEM (% WIN 55,212-2)	
Δ^9-THC	6.60 ± 0.11 (250)	51 ± 3	5.94 ± 0.57 (1157)	13 (at 10 μM)	0.2
WIN 55,212-2	6.55 ± 0.06 (284)	-	7.21 ± 0.09 (62)	-	4.6
4 (RCS-2-C4)	6.75 ± 0.13 (178)	81 ± 8	8.35 ± 0.05 (4.5)	102 ± 3	39.6
5 (RCS-3-C4)	6.48 ± 0.05 (333)	70 ± 3	7.97 ± 0.05 (11)	97 ± 2	31.2
6 (RCS-4-C4)	6.24 ± 0.08 (574)	71 ± 4	7.87 ± 0.04 (14)	96 ± 2	42.2
7 (RCS-2)	7.27 ± 0.09 (54)	93 ± 6	8.16 ± 0.04 (6.9)	98 ± 3	7.8
8 (RCS-3)	6.95 ± 0.05 (112)	99 ± 3	7.46 ± 0.06 (35)	97 ± 4	3.2
9 (RCS-4)	6.84 ± 0.06 (146)	88 ± 4	7.34 ± 0.09 (46)	87 ± 4	3.2

[a]CB_2 selectivity expressed as the ratio of CB_1 EC_{50} to CB_2 EC_{50}

hCB1 human CB_1 receptor, *hCB2* human CB_2 receptor, $pEC_{50} \pm SEM$ negative logarithm of the $EC_{50} \pm$ standard error of the mean, $Max \pm SEM$ the maximum drug effect as a percentage of that achieved by a maximally effective concentration of WIN 55,212-2, EC_{50} concentration giving 50% of the maximum drug effect

Figure 1

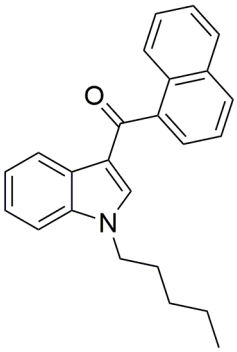

JWH-018 (**1**)

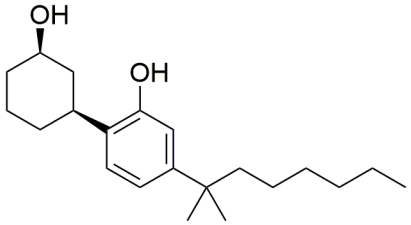

CP 47,497 (**2**)

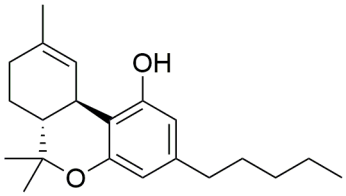

Δ^9-THC (**3**)

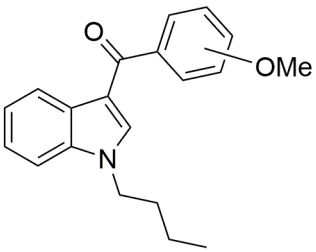

4 (RCS-2-C4): 2-OMe
5 (RCS-3-C4): 3-OMe
6 (RCS-4-C4): 4-OMe

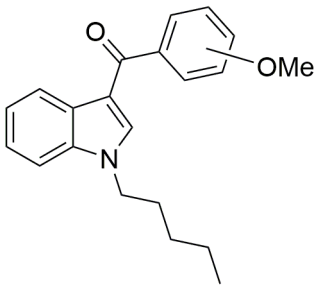

7 (RCS-2): 2-OMe
8 (RCS-3): 3-OMe
9 (RCS-4): 4-OMe

Figure 2

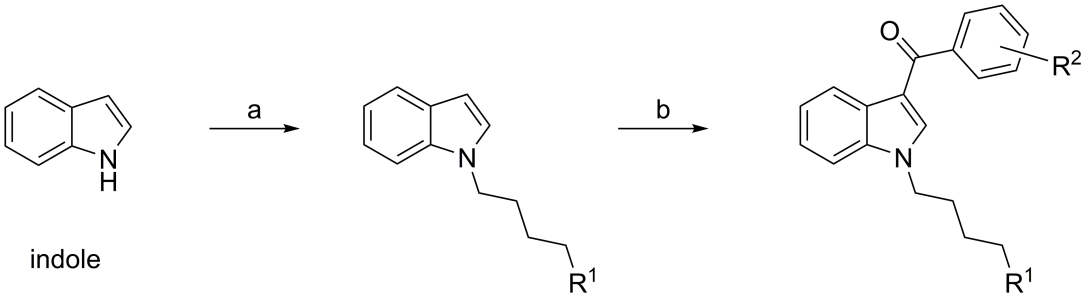

indole

10: $R^1 = H$
11: $R^1 = CH_3$

4 (RCS-2-C4): $R^1 = H$; $R^2 = 2\text{-}OCH_3$
5 (RCS-3-C4): $R^1 = H$; $R^2 = 3\text{-}OCH_3$
6 (RCS-4-C4): $R^1 = H$; $R^2 = 4\text{-}OCH_3$
7 (RCS-2): $R^1 = CH_3$; $R^2 = 2\text{-}OCH_3$
8 (RCS-3): $R^1 = CH_3$; $R^2 = 3\text{-}OCH_3$
9 (RCS-4): $R^1 = CH_3$; $R^2 = 4\text{-}OCH_3$

Figure 3

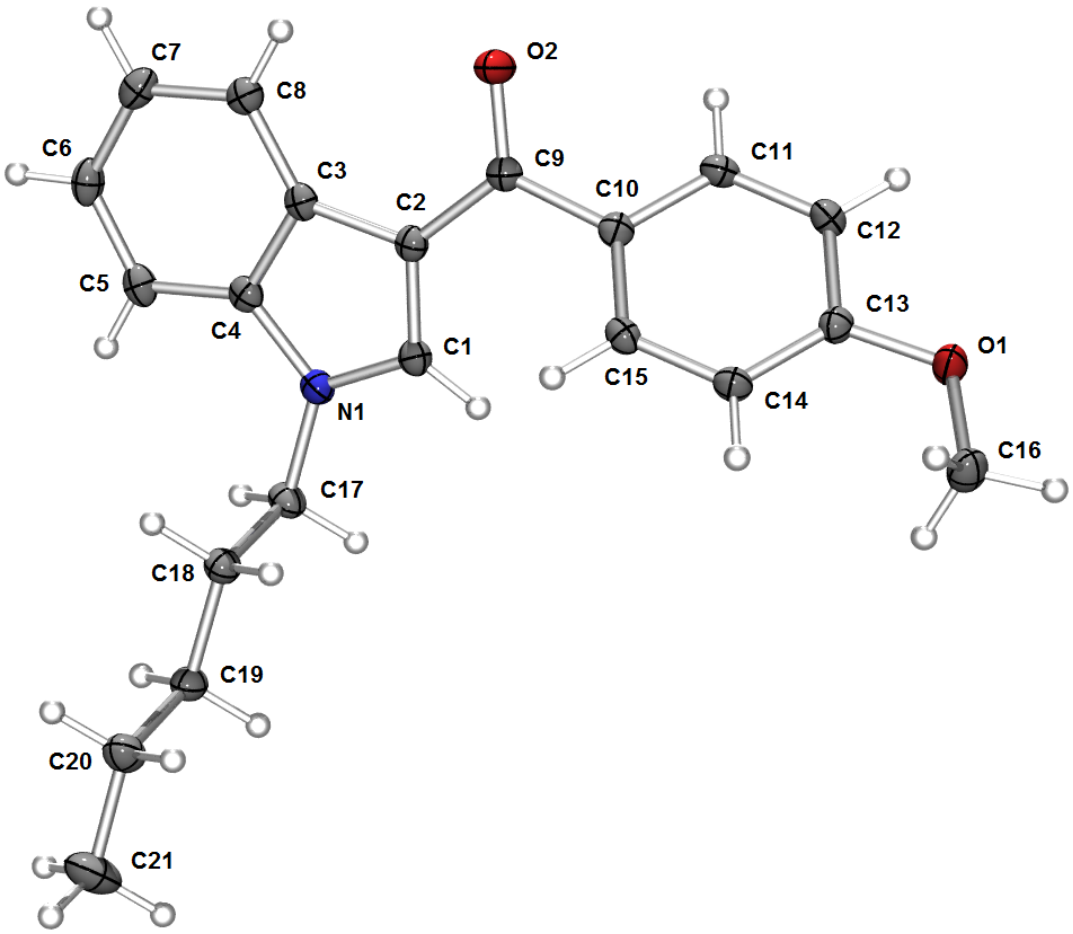

Figure 4

(a) RCS-2-C4 TIC and EI MS

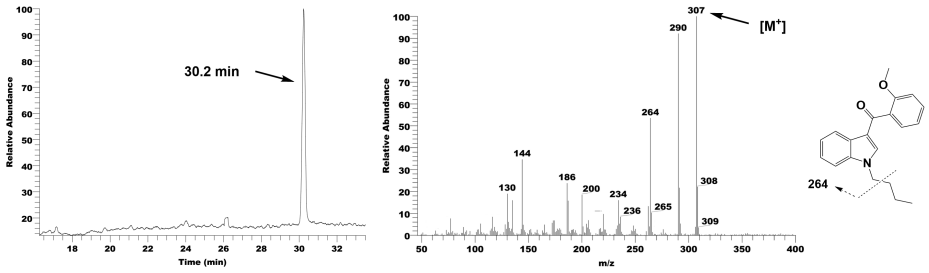

(b) RCS-3-C4 TIC and EI MS

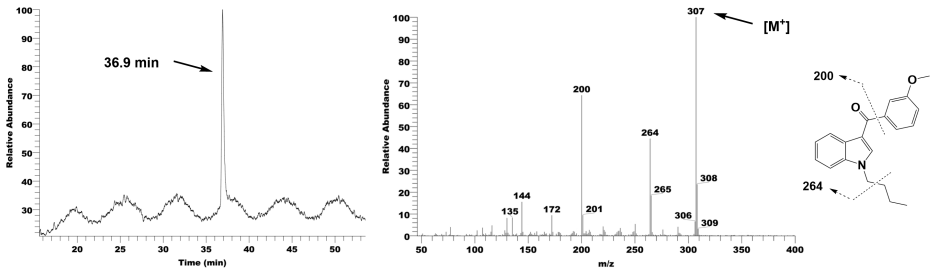

(c) RCS-4-C4 TIC and EI MS

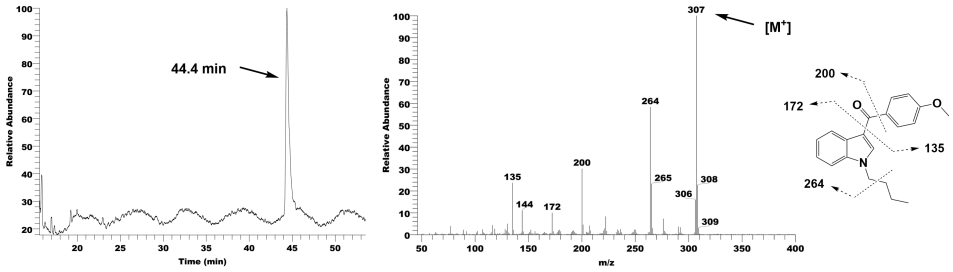

(d) RCS-2 TIC and EI MS

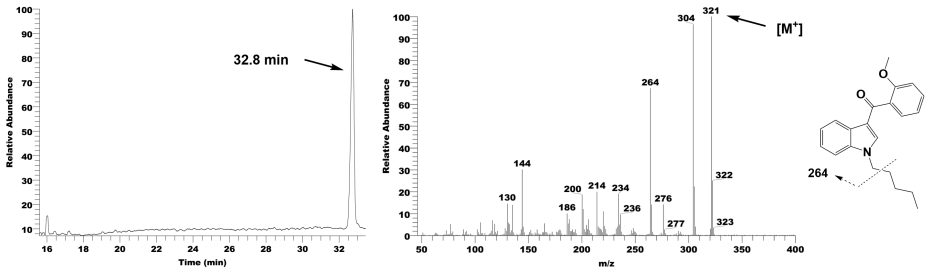

(e) RCS-3 TIC and EI MS

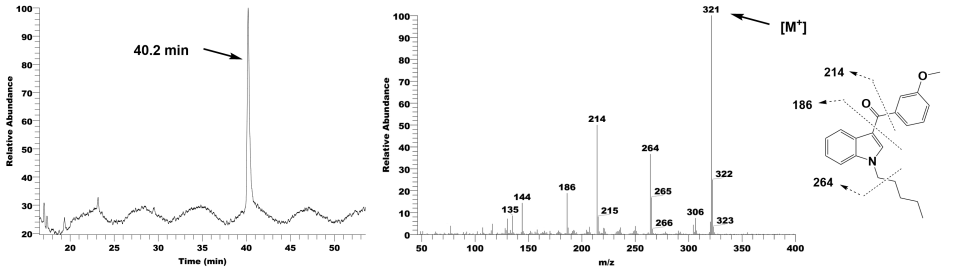

(f) RCS-4 TIC and EI MS

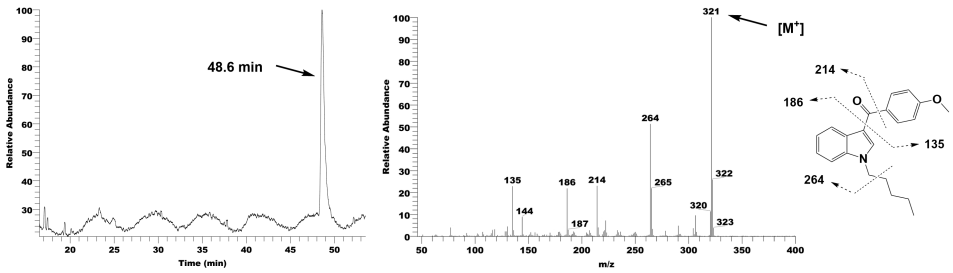

Figure 5

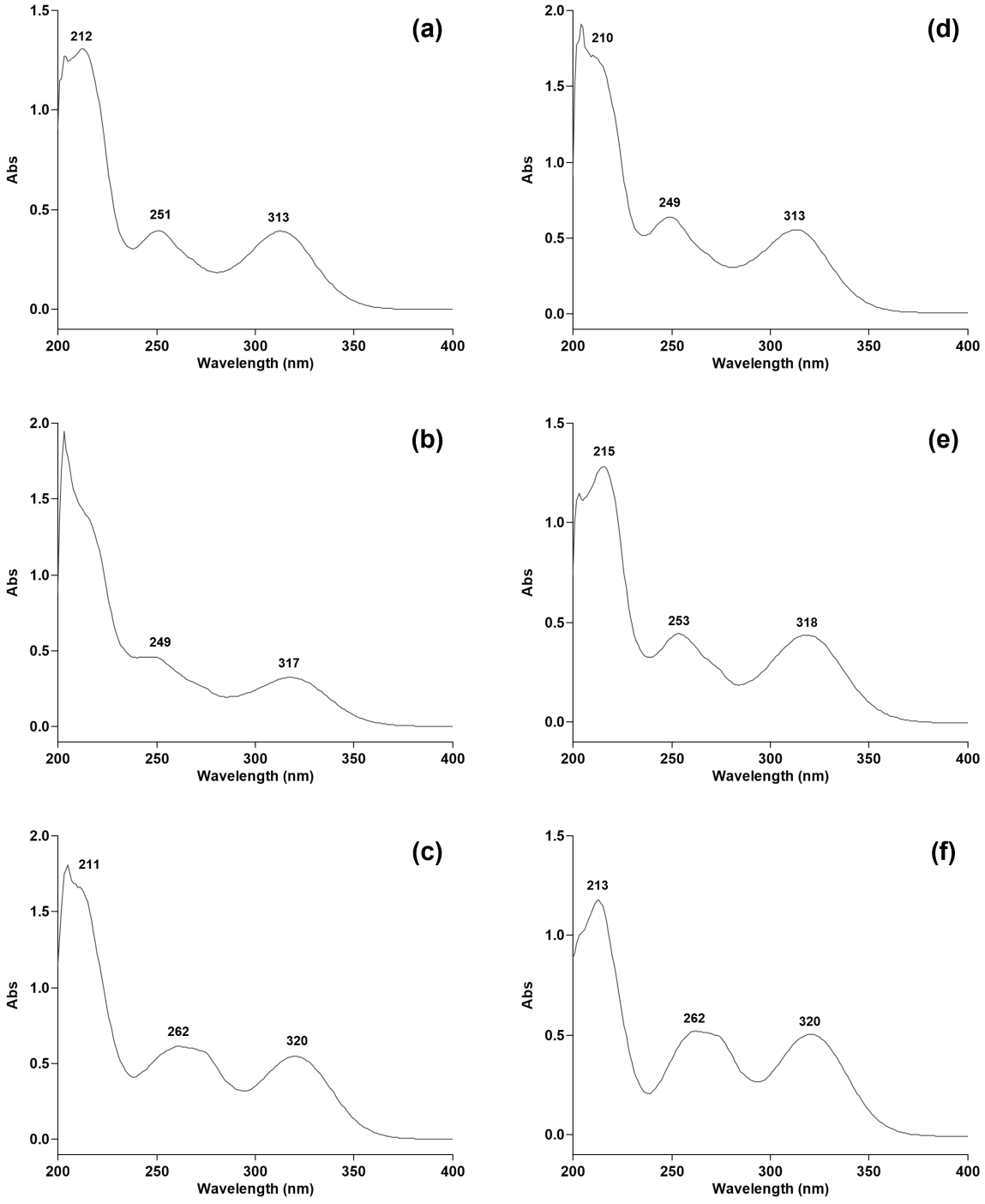
(a)
212
251
313
(d)
210
249
313
(b)
249
317
(e)
215
253
318
(c)
211
262
320
(f)
213
262
320
Abs
Wavelength (nm)

Figure 6

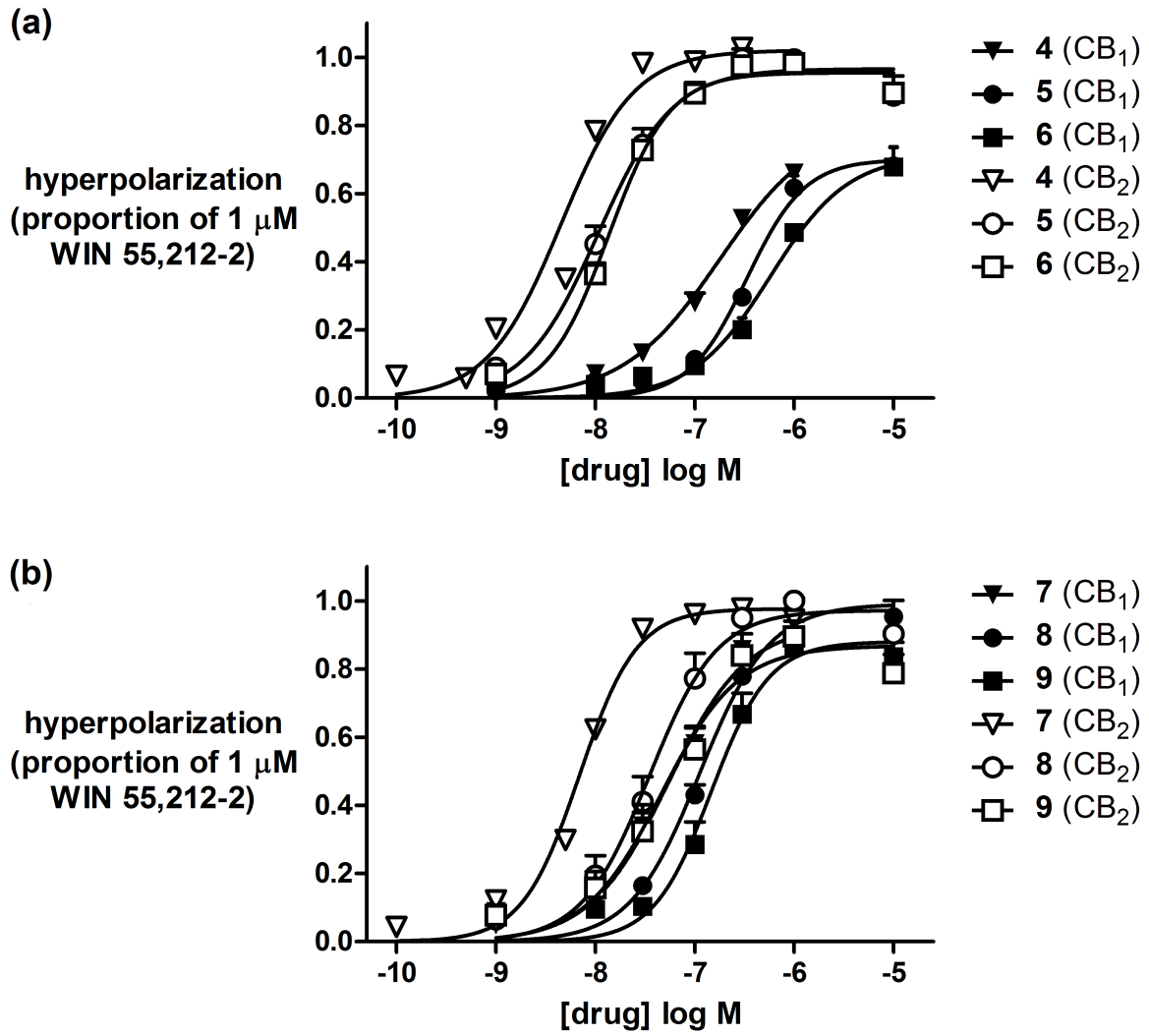
(a)
hyperpolarization
(proportion of 1 μM
WIN 55,212-2)
1.0
0.8
0.6
0.4
0.2
0.0
-10
-9
-8
-7
-6
-5
[drug] log M
4 (CB1)
5 (CB1)
6 (CB1)
4 (CB2)
5 (CB2)
6 (CB2)
(b)
hyperpolarization
(proportion of 1 μM
WIN 55,212-2)
1.0
0.8
0.6
0.4
0.2
0.0
-10
-9
-8
-7
-6
-5
[drug] log M
7 (CB1)
8 (CB1)
9 (CB1)
7 (CB2)
8 (CB2)
9 (CB2)